

Tomographic Photoacoustic Imaging Using Capacitive Micromachined Ultrasonic Transducer (CMUT) Technology

Srikant Vaithilingam *, Ira O. Wygant *, Scott Sifferman *, Xuefeng Zhuang *, Yukio Furukawa *, Ömer Oralkan *, Shay Keren †, Sanjiv S. Gambhir † and Butrus T. Khuri-Yakub*
*Edward L. Ginzton Laboratory, Stanford University, Stanford, CA 94305-4088, USA
† Department of Radiology, Molecular Imaging Program, Stanford University, Stanford, CA 94305-5105, USA

Abstract—Photoacoustic imaging is performed using a two-dimensional array of capacitive micromachined ultrasonic transducers (CMUTs) with integrated front-end electronics. Advantages of CMUT technology for photoacoustic imaging include the ease of integration with electronics, ability to fabricate large arrays with arbitrary geometries, wide-bandwidth arrays and high-frequency arrays. One of the goals of this research is to build a complete photoacoustic imaging system with an inward-looking cylindrical array that can enclose the target. As steps toward this goal two experiments are presented in this paper - photoacoustic imaging with planar scanning of the target and photoacoustic imaging with circular scanning of the target. Pulse-echo and photoacoustic images are presented. Image resolution and sensitivity of the setup are discussed and photoacoustic images of chicken tissue ablation are shown.

I. INTRODUCTION

Photoacoustic imaging has been extensively studied and notable results have been published for the imaging of humans and small animals [1]–[3]. To perform quality photoacoustic imaging, the acoustic transducer should provide good axial and lateral resolution, have high sensitivity and wide bandwidth, and should ideally acquire a whole three-dimensional (3D) image at one shot, without scanning, at fast frame rates [4]. These requirements partially contradict each other (i.e. resolution and sensitivity) or are limited by current technology (3D acquisition and transparency to laser pulse).

In this work we propose using a CMUT array to overcome some of these limitations. CMUTs typically have wider bandwidths than comparable piezoelectric transducers. This is especially significant given the broadband nature of the laser-generated ultrasound. Since CMUTs can be integrated with electronics, the parasitics in the electronics are reduced thus improving noise performance and image quality. Previous photoacoustic imaging work has typically relied on a single mechanically scanned focused piezoelectric transducer for detection of the laser-generated ultrasound. Using a CMUT array in place of a mechanically scanned element has a number of advantages. 3D images can be acquired in one shot using large two-dimensional arrays with integrated electronics. Leveraging the advantages of CMUT technology, it is also possible to build a complete inward-looking cylindrical imaging system that can enclose the target such as a small animal (Fig. 1a) A cylindrical view is better than a planar view as reconstruction

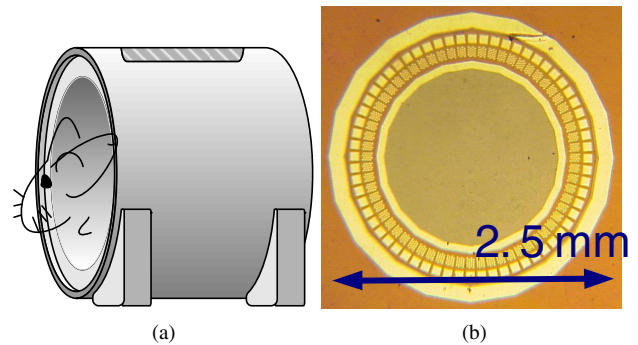


Fig. 1: (a) Diagram illustrating an inward-looking cylindrical transducer array. (b) Photograph of annular CMUT array.

artifacts can occur due to incomplete sampling from a limited planar view [5]. Arbitrary CMUT array geometries such as the ring array (Fig. 1b) have been demonstrated [6]. Flexible CMUT arrays are also currently being investigated [7]. As steps toward this complete imaging system two particular experiments were carried out - planar scanning of the target and circular scanning of target.

II. CMUT AND INTEGRATED ELECTRONICS

The transducer array used in these experiments consists of 256 elements (16 x 16). Each element is $250 \mu\text{m} \times 250 \mu\text{m}$. Thus, the entire array size is 4 mm x 4 mm. Two different sets of arrays were used - planar scanning was done with an array at a center frequency of 5 MHz while circular scanning was done at 3 MHz. The CMUT array was fabricated using surface micromachining with membranes made of silicon nitride. A more thorough description of the design and fabrication of the CMUT array has been reported elsewhere [8]. A description of the CMUT array and integrated electronics has also been previously reported [9]. The transducer array is flip-chip bonded to a custom-designed integrated circuit (IC) that comprises the front-end circuitry. Each transducer element is connected to its own amplifier via a $400 \mu\text{m}$ long through-wafer via. Integrating the electronics in this manner mitigates the effect of parasitic cable capacitance and simplifies connecting the transducer array to an external system. The IC, currently allows, for the selection of a single element at a time. Thus,

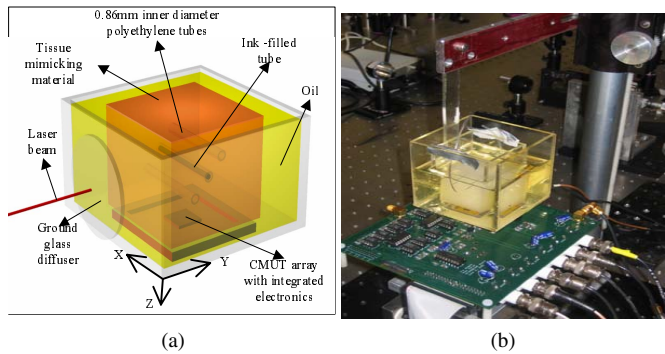


Fig. 2: Experimental setup: (a) Vessel-like photoacoustic imaging phantom. Three 0.86 mm inner diameter tubes are inside a block of tissue mimicking material. The center tube is filled with ink to provide optical contrast. The phantom is illuminated by a laser from the side. (b) Photograph of the phantom and tank. The transducer array is located at the bottom of the tank.

256 pulses are required to acquire a single image with no averaging.

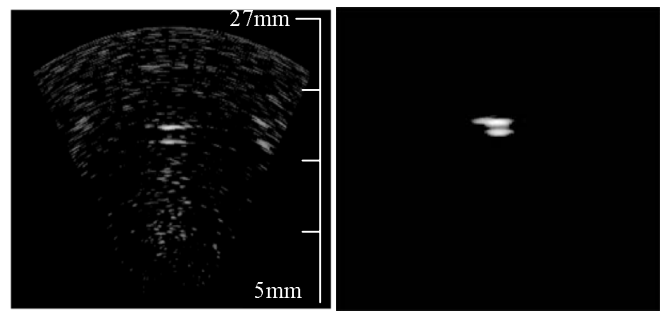
III. PLANAR SCANNING OF CMUT ARRAY

A. Experimental Setup

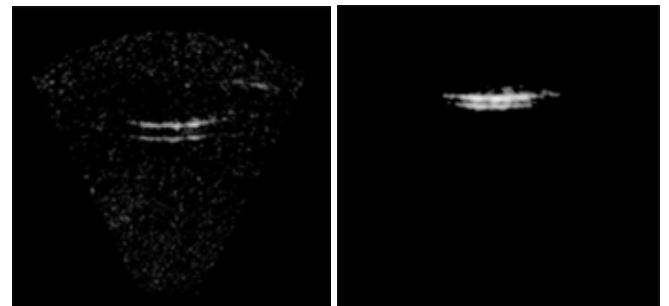
A diagram illustrating the experimental setup is shown in Fig. 2a. More details on this particular experiment have been previously reported [10]. To perform planar scanning, the CMUT array was located at the bottom of the tank on top of an X-Y translational stage. The phantom was illuminated from the side of the tank by a Q-switched Nd:YAG laser with a $1.064 \mu\text{m}$ wavelength and 12 ns FWHM pulse duration. The energy of each laser pulse was 2.3 mJ, fired at a rate of 10 Hz. A photograph of the phantom and tank is shown in Fig. 2b. After one data set was acquired, the array was translated 4 mm (length of the array) along the x-direction and another data set was acquired. Further data sets were obtained by also translating 4 mm along the y-direction. In this manner 9 data-sets were acquired. The image reconstructed from this is equivalent to an image taken with an array of size 48×48 elements.

B. Results

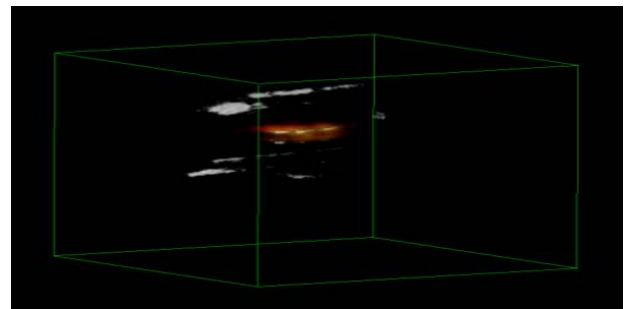
Conventional pulse-echo imaging data and photoacoustic imaging data were acquired for the phantom. Photoacoustic data was acquired by recording an element's output after the laser excitation. Images from a single scan are shown in Fig. 3a and Fig. 3b, while images constructed from planar scanning are shown in Fig. 3c and Fig. 3d. Images from planar scanning have increased clarity and the larger aperture allows the curvature of the tube to be seen. Both the photoacoustic image and pulse-echo image are constructed using a standard delay and sum image reconstruction algorithm. A 3D image of the photoacoustic image overlaid on the pulse-echo image is shown in Fig. 3e. The ink is shown as a reddish glow over the middle tube.



(a) Single scan, pulse-echo, 20 dB (b) Single scan, photoacoustic, 15 dB



(c) Planar scan, pulse-echo, 25 dB (d) Planar scan, photoacoustic, 20 dB



(e) 3D volume rendered fusion of pulse-echo and photoacoustic images. Photoacoustic data shown in red color.

Fig. 3: Images from planar scanning of CMUT Array.

IV. CIRCULAR SCANNING OF CMUT ARRAY

A. Experimental Setup

A diagram illustrating the experimental setup is shown in Fig. 4a. For these experiments, the target to be imaged was suspended in an oil tank of size $10 \text{ cm} \times 6 \text{ cm} \times 6 \text{ cm}$. Different kinds of targets were used. For example, one of the targets consisted of two polyethylene tubes of 0.38 mm inner diameter (Fig. 5b) that were embedded in a $6 \text{ cm} \times 4 \text{ cm} \times 4 \text{ cm}$ block of tissue mimicking material. The tubes were filled with India-ink to provide optical contrast. The CMUT array, located on the side of the tank, was attached to translational, tilt and rotational stages (Fig. 5a) so as to allow alignment of the array to the axis of rotation. Proper alignment makes image reconstruction easier and improves signal to noise ratio. The phantom was illuminated in a direction orthogonal to the transducer array by a Q-switched Nd:YAG laser. The laser beam was focused to a diameter of approximately 1.2 cm. The laser had a $1.064 \mu\text{m}$

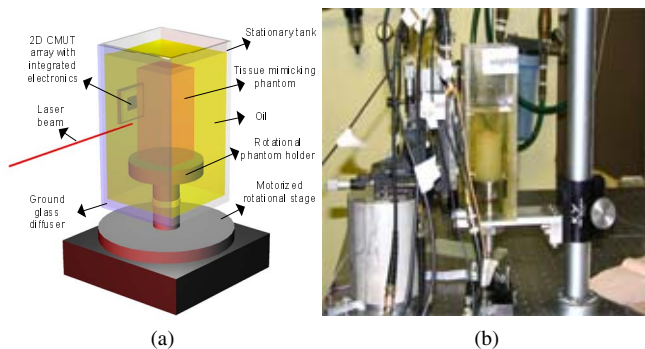


Fig. 4: Experimental Setup: (a) The phantom is illuminated by a laser from the side. (b) Photograph of the phantom and tank. The transducer array is located at the side of the tank.

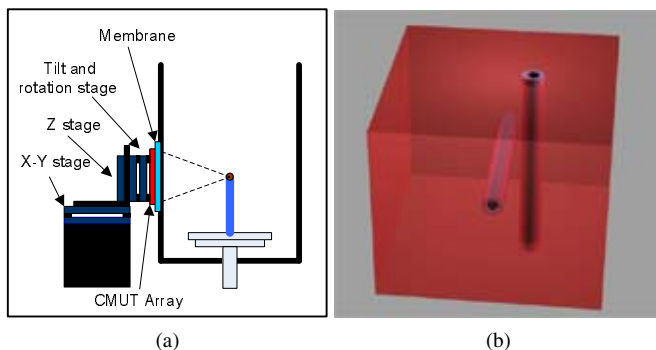
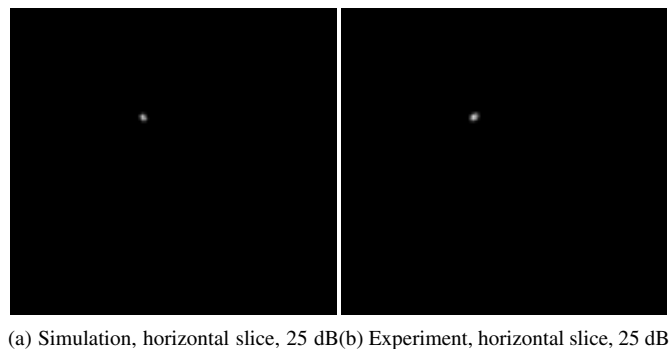


Fig. 5: (a) Alignment of the array to the axis of rotation improves image quality. (b) Sample phantom - 2 tubes of ink are placed perpendicular to each other.

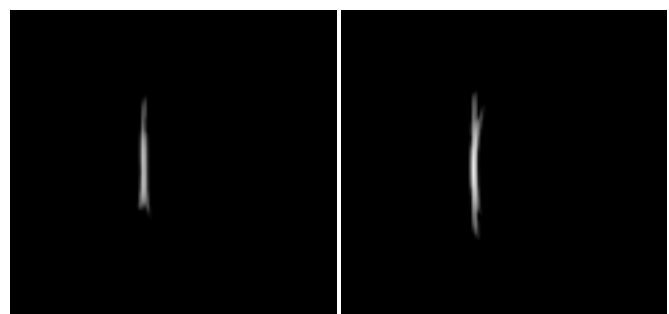
wavelength, 12 ns FWHM pulse duration and was fired at a rate of 20 Hz with energy of 13 mJ per pulse. A photograph of the phantom and tank is shown in Fig. 4b. After one data set was acquired, the target was rotated a few degrees before another data set was taken with the array. In all, the target was rotated 360 degrees in 56 steps, thus simulating a cylindrical array that is inward looking. The radius of the circle was about 3.4 cm. 2D and 3D images were then reconstructed using the complete 360 degrees of data.

B. Results

First, to verify the setup, a point target comparison was made between simulation and experiment. These results (Fig. 6) show good agreement, corroborating the alignment of the array. The horizontal resolution was found to be $350 \mu\text{m}$ at the 3dB cutoff, while the vertical resolution was 4 mm. The poor vertical resolution is due to the fact that the target was imaged at a radius of 3.4 cm corresponding to an f-number of about 8. To improve vertical resolution, vertical stepping of the array was carried out. The target in Fig. 5b was imaged once in a single rotation and once with a double rotation with the CMUT array being stepped 4 mm (height of the array) in the vertical direction for the second rotation. The results shown in Fig. 7 clearly demonstrate the improvement in vertical reso-



(a) Simulation, horizontal slice, 25 dB (b) Experiment, horizontal slice, 25 dB



(c) Simulation, vertical slice, 25 dB (d) Experiment, vertical slice, 25 dB

Fig. 6: Point target comparison between simulation and experiment shows good agreement.

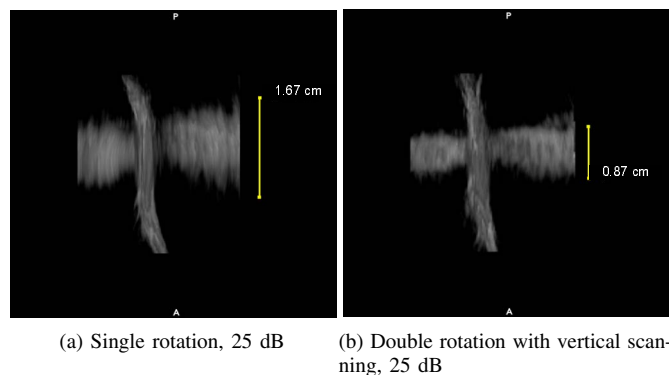


Fig. 7: These 3D volume rendered images show the improvement in vertical resolution that results from vertical scanning.

lution. Finally, chicken tissue that was embedded in phantom gel was imaged before and after ablation. The photoacoustic images along with their corresponding photographs are shown in Fig. 8. These images show promise that tissue ablation can be detected with photoacoustic tomography.

V. SENSITIVITY MEASUREMENTS

The sensitivity of the tomographic setup was also investigated. A 0.38 mm inner diameter polyethylene tube filled with India-ink was placed at the center of a tissue mimicking material. This phantom was placed on the axis of rotation, so that the tube was 3.4 cm away from the CMUT array. The concentration of India-ink was varied by powers of 1/2 and images were taken. A simple integration of the pixel values

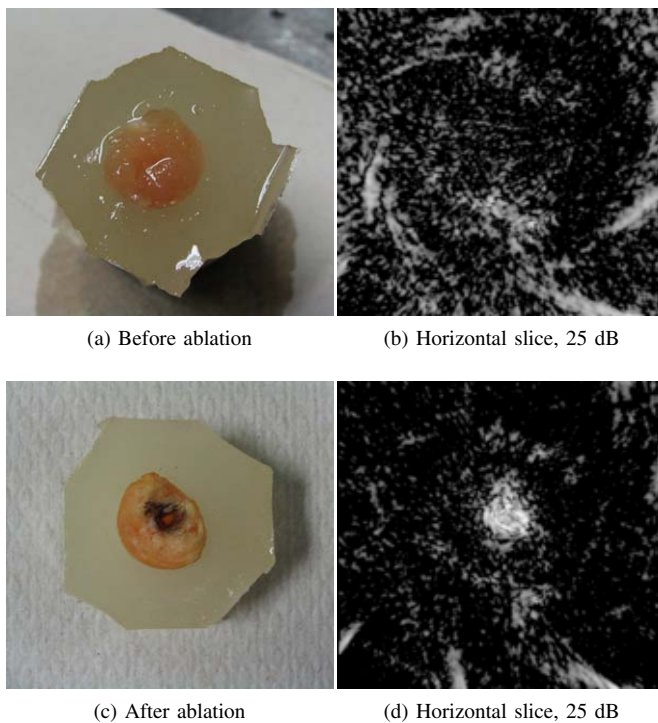


Fig. 8: Functional Imaging example - chicken tissue ablation.

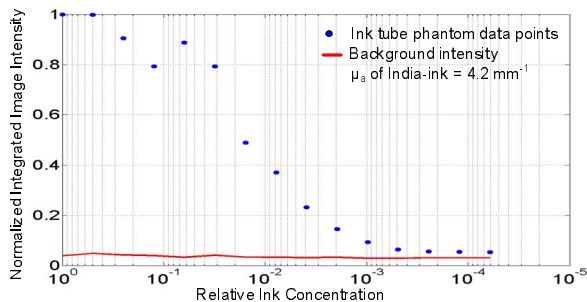


Fig. 9: Graph of normalized integrated image intensity against ink concentration.

in a volume surrounding the ink-tube was performed on each image. These values were then normalized. Results from this experiment are summarized in the graph shown in Fig. 9.

VI. ONGOING WORK

Current work is focused on imaging contrast agents like Indocyanine Green (ICG), gold nanospheres and protein-based agents. Increasing the laser power and using a tunable laser are also being investigated. Rotation of the target while stepping in the vertical direction is being implemented due to the improved vertical resolution resulting from it. Preliminary results from imaging tubes containing ICG with a laser emitting 100mJ per pulse at 690nm is shown in Fig. 10.

VII. CONCLUSION

Photoacoustic images obtained using a CMUT transducer array with integrated electronics are presented. Two different methods of imaging were studied - planar scanning and

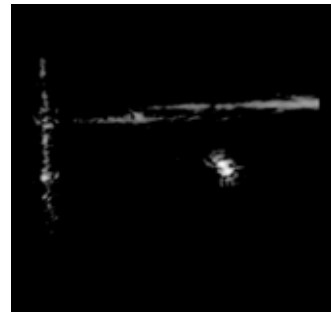


Fig. 10: Horizontal slice through phantom of perpendicular tubes containing ICG. Shown at 25 dB dynamic range.

circular scanning. Sensitivity and image resolution were also investigated. These results demonstrate some of the advantages and future potential of CMUT technology for photoacoustic imaging - in particular, the promise of building a complete cylindrical imaging system.

ACKNOWLEDGMENT

This work was supported by funds from Canon Inc. and the National Institutes of Health. The authors would like to thank National Semiconductor for the fabrication of the integrated circuits. Larry Randall provided valuable support for machining the experimental equipment. Srikant Vaithilingam is supported by a P. Michael Farmwald Stanford Graduate Fellowship. Xuefeng Zhuang is supported by a Weiland Family Stanford Graduate Fellowship.

REFERENCES

- [1] L. Wang, "Ultrasound-mediated biophotonic imaging: a review of acousto-optical tomography and photo-acoustic tomography," *Journal of Disease Markers*, vol. 19, pp. 123–138, 2004.
- [2] C. G. A. Hoelen, *et al.*, "Three-dimensional photo-acoustic imaging of blood vessels in tissue," *Optics Letters*, vol. 23, pp. 648–650, 1999.
- [3] J. J. Niederhauser, *et al.*, "Combined ultrasound and optoacoustic system for real-time high-contrast vascular imaging *in Vivo*," *IEEE Trans. Med. Imag.*, vol. 24, no. 4, pp. 436–440, 2004.
- [4] J. J. Niederhauser, M. Jaeger, and M. Frenz, "Real-time three-dimensional optoacoustic imaging using an acoustic lens system," *Applied Physics Letters*, vol. 85, no. 5, pp. 846–848, 2004.
- [5] M. Xu and L. V. Wang, "Analytic explanation of spatial resolution related to bandwidth and detector aperture size in thermoacoustic or photoacoustic reconstruction," *Phy. Rev. E*, vol. 67, p. 056605, 2003.
- [6] D. T. Yeh, *et al.*, "3-d ultrasound imaging using forward viewing cmur ring arrays for intravascular and intracardiac applications," ser. IEEE International Ultrasonics Symposium, Rotterdam, The Netherlands, Sept. 2005.
- [7] X. Zhuang, IEEE MEMS Conference, 2007, to be published.
- [8] X. Zhuang, *et al.*, "Two-dimensional capacitive micromachined ultrasonic transducer (cmur) arrays for a miniature integrated volumetric ultrasonic imaging system," in *Medical Imaging: Ultrasonic Imaging and Signal Processing*, ser. Proc. SPIE, W. F. Walker and S. Y. Emelianov, Eds., vol. 5750, 2005, pp. 37–46.
- [9] I. O. Wygant, *et al.*, "A miniature real-time volumetric ultrasound imaging system," in *Medical Imaging: Ultrasonic Imaging and Signal Processing*, ser. Proc. SPIE, W. F. Walker and S. Y. Emelianov, Eds., vol. 5750, 2005, pp. 26–36.
- [10] S. Vaithilingam, *et al.*, "Capacitive micromachined ultrasonic transducers (cmuts) for photoacoustic imaging," ser. Proc. SPIE, A. A. Oraevsky and L. V. Wang, Eds., vol. 6086, 2006, p. 608603.